Thermochimica Acta 486 (2009) 71–76

Contents lists available at ScienceDirect

Thermochimica Acta

journal homepage: www.elsevier.com/locate/tca

Thermal stability investigation of organo-acid-activated clays by TG-MS and *in situ* XRD techniques

Fethi Kooli*

Department of Chemistry, Taibah University, P.O. Box 30002, Al-Madinah Al-Munawwarah, Saudi Arabia

ARTICLE INFO

Article history:
Received 6 September 2008
Received in revised form
21 November 2008
Accepted 18 December 2008
Available online 30 December 2008

Keywords:
Organo-acid-activated clay
Hexadecyltrimethylammonium hydroxide
Acid-activation
Acid-activated clays
Thermal stability
Thermal decomposition
TG-MS

ABSTRACT

Organo-acid-activated clays were prepared with different surfactant contents by reaction of hexadecyltrimethylammonium hydroxide solution and acid-activated clays. The intercalated cations adopted different orientation in the interlayer spacing of the acid-activated clays and their thermal stability depended on the up taken amounts, acidity of the clay sheets and on the heating temperatures. The thermal stability of these materials was investigated using TG-MS, and followed by the *in situ* X-ray diffraction in nitrogen atmosphere. The clay sheets affected the decomposition of the surfactants, and as per consequence the thermal stability of the surfactants. TG-MS revealed that different types of water molecules were detected during the heating process with additional CO_2, alkanes and alkenes species at temperatures above 200 °C. The interlayer spacing collapsed after completed degradation of the intercalated surfactants.

1. Introduction

The modification of the negatively charged surfaces of clay minerals with organic cations, produces an organoclay (OCs) structure. The clay mineral becomes organophilic in character and can be used to remove hydrophobic contaminants from water [1]. Organoclays are often prepared using quaternary ammonium cations of the general form $[(CH_3)_3NR]^+$ or $[(CH_3)_2NRR']^+$ where R and R′ are hydrocarbon groups [2]. The most commonly used quaternary ammonium cation is hexadecyltrimethylammonium ion (with $R = C_{16}H_{33}$, $C16TMA^+$) where the tail group has found to have higher affinity for the exchange sites on clays relative to other surfactants [3–7]. On the other hand, the hydrophilic properties of the natural clays make them difficult to be intercalated with monomers or polymers without being modified by cationic surfactants [8]. The alkyl ammonium cations are also used for this type of modification. The organic ammonium pendent group on these exchanged cations renders the layered silicate hydrophobic, promotes the exfoliation of layered silicates and makes them compatible with the polymer matrix and forms nanocomposite samples [9]. The nanocomposites usually exhibit improved performance properties compared to conventional composites, owing to their unique phase morphology and improved interfacial properties [10,11]. The low stability of ammonium surfactants presents a problem for the melt intercalation and bulk processing of polymer nanocomposites, where high processing temperatures exceeding 200 °C are commonly used. The thermal degradation during processing could initiate/catalyze polymer degradation, in addition to cause a variety of undesirable effects during processing and in final product [12]. Efforts have been made to synthesize thermally stable organoclays based on different cations such as stibonium [13], or imidazolium [14] and phosphonium surfactants [15].

The chemical reactivity of the parent aluminosilicate affected the stability of the organoclays. The degradation of bound surfactants can be facilitated by the proximity to the catalytically active aluminosilicates sites [16]. This reactivity could be modified by acid-activation. The acid treatment led to chemical leaching of some cations from clay sheets accompanied with an increase of surface area and enhances the acidity of the obtained clays [17]. In this regards, we were interested to prepare organoclays from different acid-activated clays to prepare stable porous clay heterostructures with enhanced acidity [18]. The acid-activated clays (OAACs) exhibited different intercalation properties compared to the nonacid-treated raw clay [19]. The thermal stability of the organo-acid-activated clays (OAACs) was related to the amount of up taken surfactants and to acid-activation level. The organoclay prepared from a clay treated at higher acid to clay ratios exhibited higher thermal stability compared to the one prepared from a clay treated at lower acid/clay ratios [20]. The layered structure of OAACs were maintained in the range of 200–400 °C with

* Tel.: +966 8460008x1405; fax: +966 48470235.
E-mail address: fkooli@taibahu.edu.sa.

0040-6031/$ – see front matter © 2009 Elsevier B.V. All rights reserved.
doi:10.1016/j.tca.2008.12.025

a basal spacing varying from 3 to 4 nm, as indicated by *in situ* XRD taken at reel temperature without cooling the samples [20]. The temperatures at which the *in situ* XRD was performed, were deduced from thermogravimetric analysis (TG) curves. The thermogravimetric analysis alone is so limited, because the chemical identification of the volatile gases is not possible. The use in conjunction with mass spectrometry will enable the identification of the evolved gases and the release temperature of alkyl degradation. The thermogravimetric analysis combined with mass spectrometry (TG-MS) was used to study the thermal degradation of organoclays [21]. To the best of our knowledge, TG-MS studies related to the OAACs were not reported. Here we investigate in detail the evolution of gaseous species from two selected OAACs with different intercalated amount of C16TMA cations, using a. TG-MS technique. The structural changes during the C16TMA decomposition was followed by *in situ* X-ray diffraction. We have tried to correlate the decomposition of the cationic surfactants with the acidity of these acid-activated clays.

2. Experimental

2.1. Materials

The raw clay (Ca-montmorillonite, STx-1) was purchased from the Source Clays repository, Purdue University (USA) and used as received. The acid-activation was performed with sulphuric acid (98%) at a fixed acid/clay ratio of 0.3 (in weight) at room temperature (Amt-RT) or at 90 °C (Amt-90), as described in our previous work [22]. The organo-acid-activated clays (OAAcs) were prepared by an exchange reaction using C16TMAOH solution. Briefly 1 g of each acid-activated clay was added to 3 g of C16TMAOH solution and 22 ml of deionized water, corresponding to a concentration of 2.47 mmol. This concentration value was selected according to our previous studies. After overnight, the samples were collected by filtration and washed with deionized water. The samples will be assigned as follows: C16TMA-Amt-RT and C16TMA-Amt-90. The sample C16TMA-mt is identified as the organoclay prepared from the starting clay without a prior acid treatment.

2.2. Characterization of organo-acid-activated clays

The elemental analysis of C, N, and H was performed using EURO EA elemental analyzer. The powder X-ray diffraction (XRD) patterns were collected on a Bruker Advance 8 diffractometer (Ni-filtered Cu Kα radiation). The *in situ* powder XRD patterns between RT and 425 °C were taken using an Anton Parr heating stage KT450, under nitrogen atmosphere at real temperature values, without cooling the samples. Thermogravimetric coupled with mass spectrometry (TG-MS) experiments were carried out using SETSYS$_{évo}$ thermoanalyzer (SETARAM instrumentation) coupled to mass spectrometer (omnistar) from pfeiffer by stainless capillary at temperature of 300 °C. The measurements were carried out in flow of dry nitrogen heated from room temperature to 900 °C, at a heating rate of 5 °C min^{-1}. Only selected gases were analyzed. The acidity of acid-activated clays was measured by using the cyclohexylamine as a probe molecule [23].

3. Results and discussion

3.1. Powder X-ray diffraction

Fig. 1 depicts the powder XRD of the two acid-activated clays and their organo-acid-activated counterparts. The Amt-90 exhibited a higher partial destruction compared to Amt-RT, with a decrease in intensity of 0 0 1 reflection and a relative increase of the amorphous

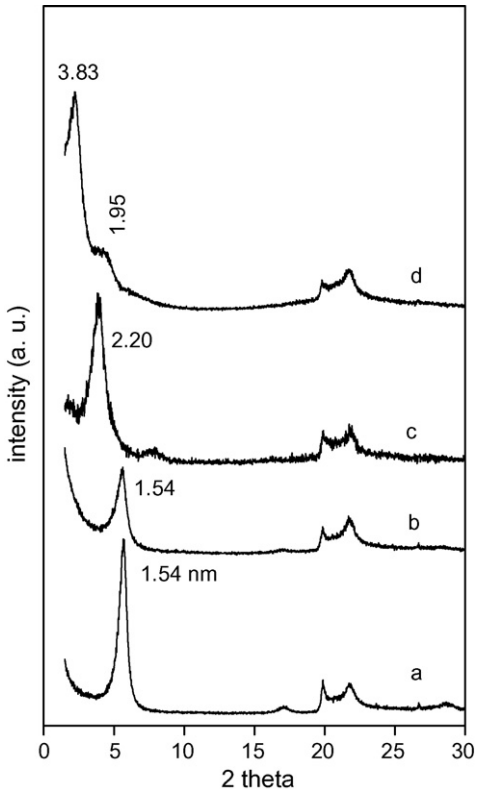

Fig. 1. Powder XRD of clay acid-activated at (a) RT and (b) 90 °C, and their organo-derivatives (c) C16TMA-Amt-RT and (d) C16TMA-Amt-90, respectively.

silica phase in the range between 25° and 30°. The intercalation of C16TMA cations was successfully achieved with an increase of the basal spacing of Amt-RT and Amt-90 clays from 1.54 to 2.20 and 3.83 nm, respectively. The significant expansion of the basal spacing from 2.20 to 3.83 nm indicates a possible transition of alkyl chain configuration from the monolayer paraffin structure (2.20 nm) to a bilayer paraffin complex (3.83 nm) [2,22]. The montmorillonite sheet thickness is 0.96 nm, and the length of the fully extended of C16TMA cations was estimated about 2.53 nm [24]. The interlayer gallery is about of 1.22 nm (deduced from the subtraction of the basal spacing of OAACs from 0.96 nm), where the intercalated molecules adopted a monolayer paraffin type arrangement where C16TMA cations were titled of 29° (degree). This value was close to that reported for a monolayer paraffin structure in the case of nonacid-activated montmorillonite [2]. While, C16TMA-Amt-90 material exhibited an interlayer gallery of 2.84 nm which exceeded the length of C16TMA cations. In this case, the cations adopted a tilted bilayer paraffin arrangement. For a simple case of a bilayer structure where methylene chains are exclusively all-*trans*, the tilt angle is about 35° with respect to the layers [22].

3.2. Elemental analysis

The validity of C, N and H elemental analysis was compared to the pure C16TMABr salt. The data indicated that Amt-90 intercalated more surfactants (1.24 mmol g^{-1}) than Amt-RT (0.84 mmol g^{-1}). These data were surprising, because the Amt-RT exhibited higher cation exchange capacity (CEC of 0.82 meq g^{-1}) compared to Amt-90 (0.74 meq g^{-1}). The up taken amount was higher than the CEC value for Amt-90. This fact indicated that the intercalation in the latter did not occur via cation exchange reaction [25], and other process could occur [20]. The pH values of the C16TMA-clay suspensions was above 10, the surface of Amt-90 clay became more negatively charged, and thus favored the adsorption of C16TMA

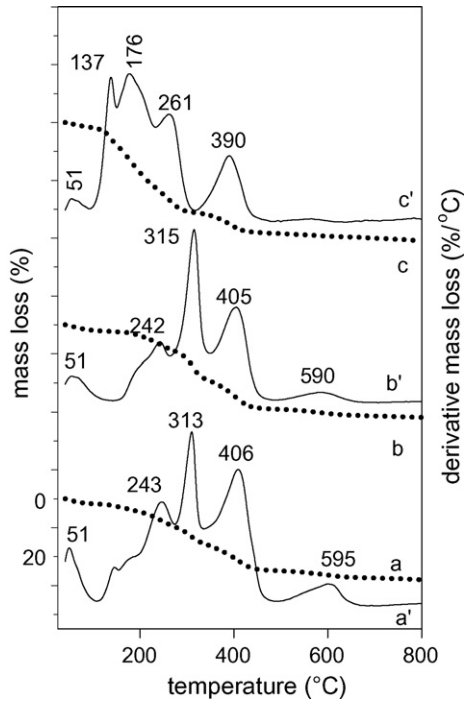

Fig. 2. TG (dotted line) and their corresponding derivatives (DTG, plain line) curves of the organo starting clay (a and a′) C16TMA-mt and the organo-acid-activated clays, (b and b′) C16TMA-Amt-RT and (c and c′) C16TMA-Amt-90, respectively.

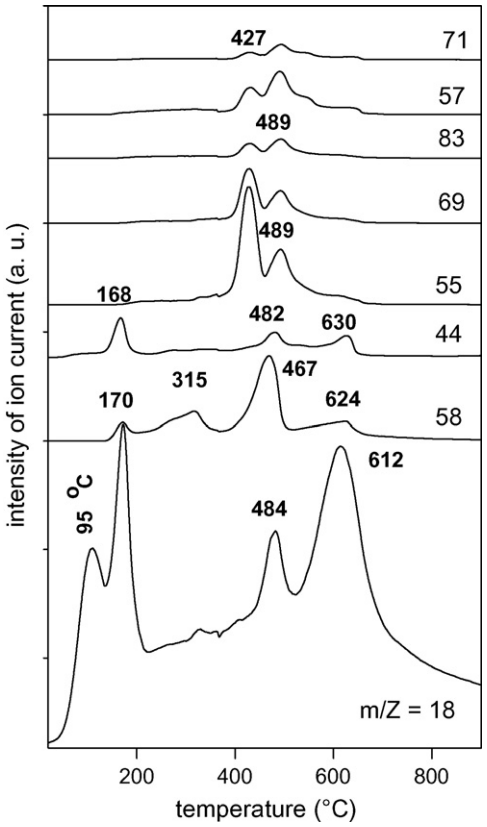

Fig. 3. MS profiles on gases from C16TMA-Amt-RT at a heating rate of 5 °C min^{-1}.

cations, due to the electrostatic interactions between the charged surface and the cationic surfactants on both sides of the clay sheets, and followed by restacking [22]. The proposed explanation was supported by our powder XRD data.

3.3. Thermogravimetric analysis

Fig. 2 shows the TG mass loss curves and the corresponding derivative curves (DTG) of the organoclay prepared from nonacid-activated clay (C16TMA-mt) and the two organo-acid-activated clays. Small mass loss at 51 °C was related to residual water molecules present in all organoclay and organo-acid-activated clays compared to the starting acid-activated clays. The C16TMA decomposition occurred in the range of 150–500 °C. The relative mass loss above 150 °C increased with surfactant content and it was in good agreement with the elemental analysis. At temperatures above 520 °C, the dehydroxylation of the clay sheets occurred, and a broad peak around 590–595 °C was observed for C16TMA-mt and C16TMA-Amt-RT samples. This peak was difficult to detect in case of C16TMA-Amt-90, due to the destruction of the clay sheets during the acid-activation at 90 °C. The feature of the organoclays was different for each sample. The C16TMA-mt and C16TMA-ACmt-RT exhibited similar features with three defined mass losses in the range of 220–500 °C, with a shoulder below 200 °C. While the C16TMA-Amt-90 showed four defined mass losses in the range of 100–500 °C. The maximum mass loss rate temperature in the range of 400 and 500 °C was higher for C16TMA-mt and C16TMA-Amt-RT (405 °C) than C16TMA-Amt-90 (390 °C, Fig. 2). This behavior may be related to the formation of carbonaceous char from the organic component in organo-acid-activated clays and their oxidative dehydrogenation which was promoted by the catalytic properties of the montmorillonite surfaces. The onset decomposition temperatures, the maximum mass loss rate temperatures for each step and the residual masses are presented in Table 1 for the acid-activated clays and their organo-derivatives. The onset degradation occurred at temperatures in the range 122–182 °C. However, the maximum mass loss rates occurred above 130 °C. The residual mass decreased with the increase of the overall surfactant content in case of C16TMA-Amt-90 compared to C16TMA-Amt-RT.

We have reported that the solid C16TMABr exhibited only one maximum mass loss rate temperature at 266 °C [20]. The position of the maximum mass loss rate temperatures for C16TMA-Amt-90 shifted to lower range compared to the C16TMA-mt, C16TMA-Amt-RT sample and to the pure C16TMABr. This fact was related to the acid sites of the acid-activated clay which have a catalytic effect on the initial stages of decomposition of the C16TMA cations within the organo-acid-activated clay treated at higher temperature. Indeed, the acidity of Amt-RT (0.54 mmol H^+ g^{-1}) was lower acidity compared to that of Amt-90 (0.68 mmol H^+ g^{-1}) measured

Table 1
Onset decomposition temperature, the maximum mass loss rate temperatures for each step and the residual masses for the acid-activated clays and their organo-acid-activated clays in nitrogen atmosphere.

Samples	Intercalated amounts	Onset decomposition temperature	Maximum mass loss rate temperatures	Residual masses
Amt-RT	–	30 °C	51, 100 °C	70%
Amt-90	–	26 °C	51, 82 °C	84%
C16TMABr	–	195 °C	266 °C	0%
C16TMA-Amt-RT	0.84 mmol g^{-1}	182 °C	242, 315, 405 °C	72%
C16TMA-Amt-90	1.24 mmol g^{-1}	122.5 °C	137, 176, 261, 390 °C	62%

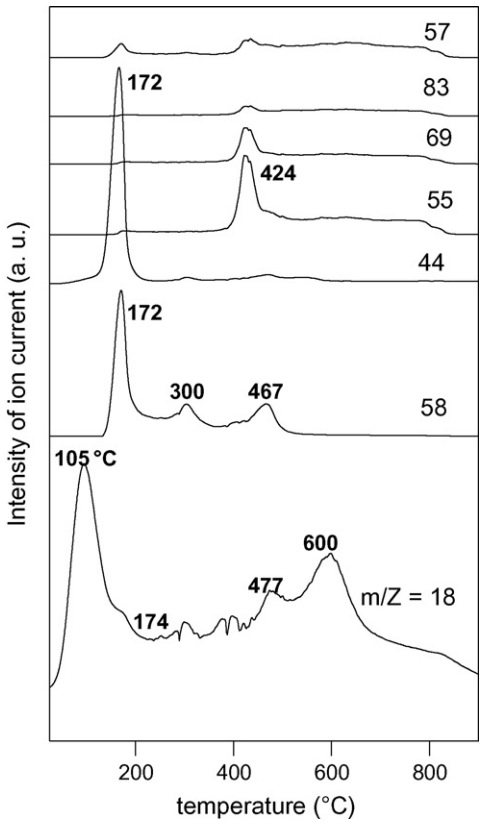

Fig. 4. MS profiles of gases from C16TMA-Amt-90 at a heating rate of 5 °C min^{-1}.

by cyclohexylamine probe molecule. In addition, the single step decomposition of C16TMABr salt compared to the multistep process within the organoclay and organo-acid clays implies that the presence of the nanoscopic dimensions of the interlayer drastically influences reaction kinetics, product transfer, and volatilization [16].

3.4. The decomposition products

The MS spectra of evolved products for C16TMA-Amt-RT is shown in Fig. 3. The water (m/z = 18) molecules were evolved at two different temperatures of 95 °C, and 170 °C, indicating the presence of two types of water in this sample, may be a physiadsorbed water on the external surface and water co-existed within the interlayer of the organoclay. The later was not observed in TG curves. The water was also detected at higher temperatures between 400 and 800 °C, due to different dehydroxylation steps of Amt-RT. In case of C16TMA-Amt-90, only one type of water was evolved at 105 °C while the DTG feature exhibited only one peak at 51 °C (Fig. 4). The intensity of these peaks at higher temperatures was lower compared to that for C16TMA-Amt-RT, and indicate that the destruction of the layers was enhanced at 90 °C compared to RT, in good agreement with our previous studies [22]. The presence of water molecules in the range of 100–180 °C suggested that with high surfactant contents it is not possible to transform the acid-activated clays into entirely "hydrophobic" material [12]. The CO_2 (m/z = 44) was produced between RT and 230 °C, with traces at higher temperature after dehydroxylation of the clay sheets in the case of C16TMA-Amt-RT. The low intensity peak of CO_2 gas in this sample could be related to the amount of intercalated C16TMA cations compared to C16TMA-Amt-90. The temperature of the CO_2 products coincided well the temperatures of the dehydroxylation of the clay sheets, evidenced by the observation of H_2O (m/z^+ = 18) from 400 to 800 °C. We noted that the presence of carbonaceous materials affected the dehydroxylation temperature of the layered silicates compared to the starting clays, and could be the origin of the CO_2 gas at higher temperatures.

The degradation of organoclays occurred via Hofmann elimination, producing olefin and an amine. The m/z numbers were selected from the studies of Xie et al. [16] $NCH_2(CH_3)_2$ (m/z = 58), alkenes (m/z = 55, 69, 83), and alkanes (m/z = 57, 71, 85) were evolved at higher temperatures between 400 and 550 °C, and indicated that the decomposition of the C16TMA cations occurred at different fragmentation steps and depended of the acidity of the host clays. The complete removal of alkyl groups occurred before the complete dehydroxylation of the clay sheets. The carbonaceous materials resulting form these products were transformed to CO_2 gas. Xie et al. [16] have reported that the formation of CO_2 occurred at higher temperatures in the range of 600–800 °C, and the metallic species within the aluminosilicate catalyzed a reaction between the carbonaceous residue and the oxygen in the crystal structure of dehydroxylated montmorillonite [16]. In our case, similar phenomena could occur but at lower temperatures due to the difference in composition of the clays which was affected by acid treatment, and/or to the acid sites resulting from the acid-activation.

In general the peak's intensity of the evolved gases were quiet higher in the C16TMA-Amt-90 compared to those of C16TMA-Amt-RT, and could be related to the surfactant amounts. Using TG-FTIR technique, Cervantes-Uc et al. [26] have reported that in addition to Hoffman elimination reaction, a new mechanism occurred included the thermal degradation of tallow residue and the thermal decomposition of un-exchanged surfactants in some commercially organoclays. The type of anion existing in the surfactant played also a key role on the thermal stability of organoclays [26].

3.5. In situ powder X-ray diffraction

The *in situ* powder XRD studies were carried out to characterize the thermal stability of the different organoclays for further use as precursor for nanocomposites. For acid-activated clay Amt-RT, a gradual decrease of basal spacing was observed from 1.54 to 1.43 nm at 50 °C, then to 1.13 nm at 100 °C. It continued to decrease to 0.98 nm at 150 °C. This phase was stable till 400 °C (Fig. 5). However, the Amt-90 exhibited two different basal spacing at 1.32 and 0.98 nm at 150 °C. The stability of the 1.32 nm phase at higher temperatures could indicate that the presence of some amorphous silica which prevented the collapse of the interlayer spacing and acted as a pillaring agent [27] (Fig. 6).

The solid C16TMABr has a lamellar ionic crystals comprised of alternating layers of paraffinic alkyl chains and of ionic groups and associated hydration water. For the first time, we have reported the *in situ* powder XRD patterns of the solid C16TMABr in nitrogen atmosphere, our data indicated a continuous increase of the basal spacing from 2.61 to 3.23 nm at intermediate temperatures in the range 150–215 °C. The entire structure was collapsed at heating temperature above 250 °C [20].

The *in situ* powder XRD of the C16TMA-Amt-RT indicated that the interlayer spacing was stable up to 200 °C with a slight variation of the basal spacing (Fig. 7). A decrease of the interlayer was observed from 1.91 to 1.44 nm in temperature range of 215–250 °C. Although the TG-MS data indicated that water and CO_2 molecules were released in this range, but it affected slightly the mobility of the intercalated surfactants. A continuous decrease up to 1.44 nm at 400 °C was detected, after complete degradation of the intercalated surfactants, and indicates that carbonaceous products were still present between the interlayer spacing of the clay sheets. Indeed, the TG-MS data showed no gases were evolved in this temperature range, except for the $N^+CH_2(CH_3)_2$ (m/z = 58) (see Fig. 3). Similar

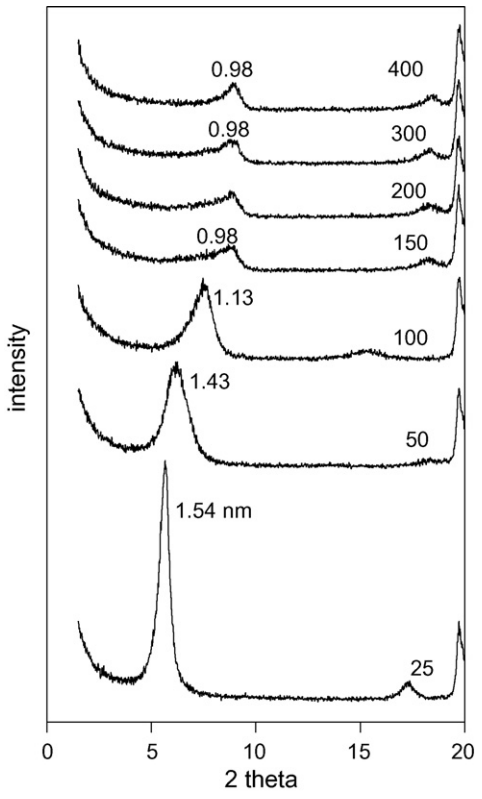

Fig. 5. *In situ* powder XRD of acid-activated clay treated at room temperature (Amt-RT) heated at different temperatures (°C).

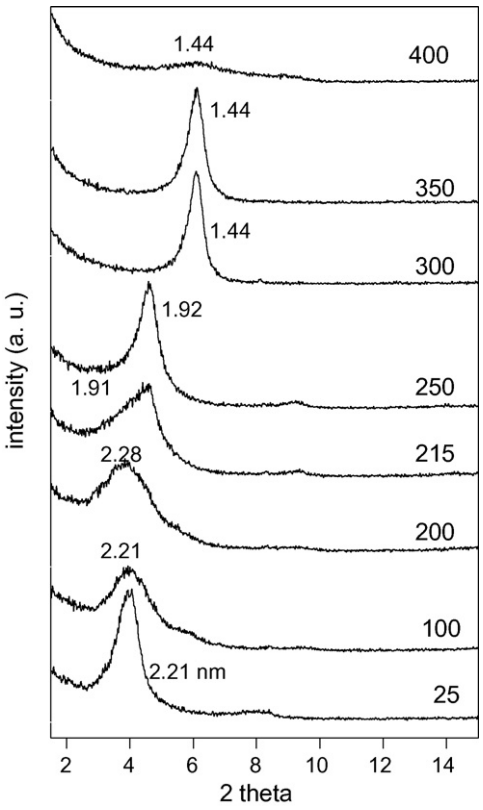

Fig. 7. *In situ* powder XRD of organo-acid-activated clay (C16TMA-Amt-RT) heated at different temperatures (°C).

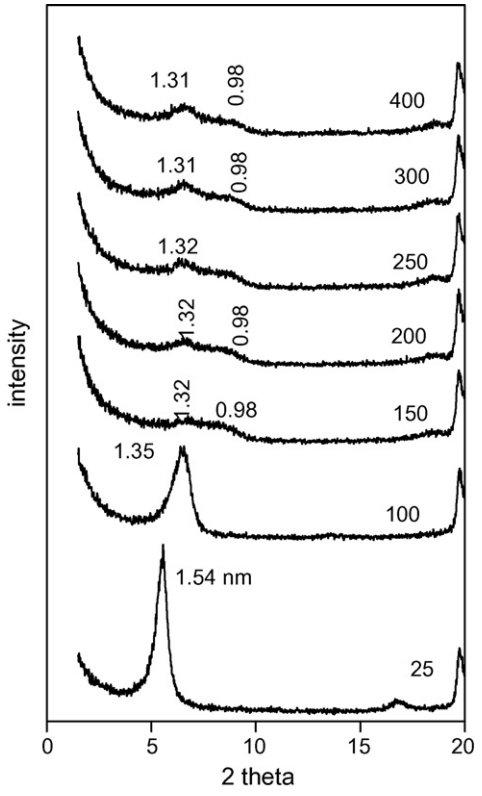

Fig. 6. *In situ* powder XRD of acid-activated clay treated at 90 °C (Amt-90) heated at different temperatures (°C).

observations were observed for the C16TMA intercalates within the raw clay and other clays [20,28].

The C16TMA-Amt-90 behaved differently, an increase of the basal spacing was observed from 4.03 to 4.22 nm at 150 °C (Fig. 8). The desorption of water did not affect the basal spacing of the organoclay, and could indicate that this water is physisorbed outside the interlayer spacing. However, the CO_2 gas could facilitate the mobility and the reorientation of intercalated C16TMA cations, which was not in the case of C16TMA-Amt-RT. The interlayer spacing was decreased to 1.95 nm at 200 °C due to the decomposition of the intercalated surfactants. The TG-MS showed that the peak maximum of $NCH_2(CH_3)_2$ ($m/z = 58$) was released at 172 °C with higher intensity compared to C16TMA-Amt-RT one, resulting from the higher content of C16TMA cations in the Amt-90 host clay. Above this temperature (i.e. 200 °C) the basal spacing continued to decrease till 1.45 and 1.35 nm from 250 to 350 °C. This value was quite higher compared to pure Amt-90 heated at the same temperature, due to the presence of carbon species between the layers, as we have mentioned above.

Previous studies related to alkylammonium smectites indicated that an initial increase of the basal spacing when heated from 50 to 100 °C occurred due to the changes from ordered pseudocrystalline structure of adsorbed surfactants bilayers to less ordered liquid crystal-like conformation [28,29]. In our case, it was difficult to observe this phenomenon as a result of possible absence of disordered conformations of the intercalated surfactants. However, the observed expansion at intermediate temperatures (100–150 °C) for C16TMA-Amt-90 could be related to the thermal expansion of C16TMA normal to the layers, after the production of volatile gases such as CO_2, inducing a development of internal pressure with the interlayer region [30]. This fact was in good agreement with the TG-MS data. However, Lee and Kim have reported that the dehydration process could induce the expansion of the interlayer spacing [31].

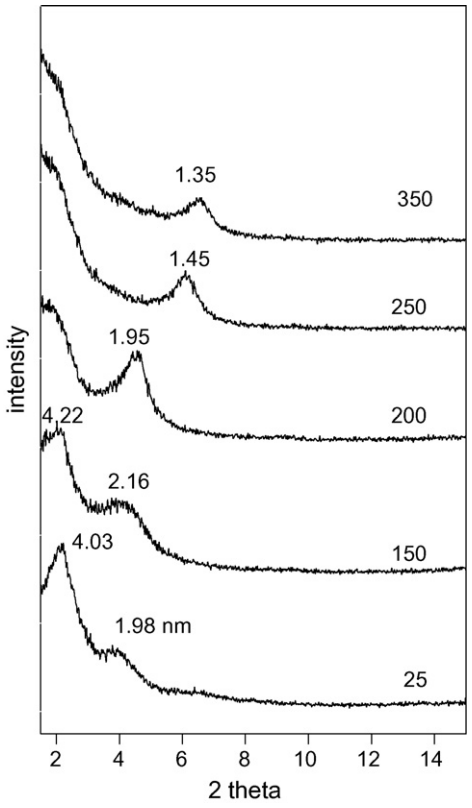

Fig. 8. *In situ* powder XRD of organo-acid-activated clay (C16TMA-Amt-90) heated at selected temperatures (°C).

In our case, the water molecules were not detected by TG-MS in this temperature range.

4. Conclusions

Organo-acid-activated clays were prepared from two different acid-activated clays. The up taken amounts of C16TMA cations and the interlayer spacing of these materials depended on the temperature of acid-activated clays at similar C16TMAOH concentration. TG data indicated that intercalated C16TMA cations were released at lower temperatures compared to the pure salt of C16TMABr. Although it believed that the organoclays were hydrophobic, in our case different types of water molecules were detected by MS and depended on the extend of acid-activation. Different species were evolved at higher temperatures during the thermal degradation of the intercalated surfactants, accompanied with a decrease of the interlayer spacing. However, at intermediate temperatures between 100 and 200 °C, the *in situ* powder XRD indicated an increase of the interlayer spacing as a result of the production of volatile gases such as CO_2 and/or the $NCH_2(CH_3)_2$.

Acknowledgements

The author would like to thank the Institute of Chemical and Engineering Sciences, Agency of Science, Technology and Research (A-star), Singapore and Taibah University (Grant 429/220) Saudi Arabia, for the financial support, and SETARAM company for the TG-MS data.

References

[1] W. Beall, Appl. Clay Sci. 24 (2003) 11–20.
[2] G. Lagaly, M. Ogawa, I. Dékány, Clay mineral–organic interactions, in: F. Bergaya, B.K.G. Theng, G. Lagaly (Eds.), Handbook of Clay Science, Elsevier, Amsterdam, 2006, pp. 309–377.
[3] G.M. Haggerty, R.S. Bowman, Environ. Sci. Technol. 28 (1994) 452–458.
[4] S.A. Boyd, M.M. Mortland, J. Soil Sci. Soc. Am. 52 (1998) 652–656.
[5] W.F. Jaynes, S.A. Boyd, J. Soil Sci. Soc. Am. 55 (1991) 43–48.
[6] S. Guangyao, X. Shihe, S. Boyd, Water Res. 30 (1996) 1483–1489.
[7] H.P. He, R.L. Frost, J.X. Zhu, Spectrochim. Acta, Part A: Mol. Biomol. Spectrosc. 60 (2004) 2853–2859.
[8] G. Lagaly, Appl. Clay Sci. 15 (1999) 1–9.
[9] C. Kato, K. Kuroda, K. Misawa, Clays Clay Miner. 27 (1979) 129–136.
[10] P.C. LeBaron, Z. Wang, T.J. Pinnavaia, Appl. Clay Sci. 15 (1999) 11–29.
[11] M. Alexandre, P. Dubois, Mater. Sci. Eng. 28 (2000) 1–63.
[12] M. Gelfer, C. Burger, A. Fadeev, I. Sics, B. Chu, B.S. Hsiao, A. Heintz, K. Kojo, S.-L. Hsu, M. Si, R. Rafailovich, Langmuir 20 (2004) 3746–3758.
[13] D. Wang, C. Wikkie, Polym. Degrad. Stab. 82 (2003) 309–315.
[14] S. Bourbigot, D. Vanderhart, J. Gilman, W. Awad, R. Davis, A. Morgan, C.J. Wikkie, Polym. Sci. Part B, Polym. Phys. 41 (2003) 3188–3213.
[15] J. Uribe Calderon, B. Lennox, M.R. Kamal, Appl. Clay Sci. 40 (2008) 90–98.
[16] W. Xie, Z.P. Gao, W. Pan, D. Hunter, A. Singh, R. Vaia, Chem. Mater. 13 (2001) 2979–2990.
[17] P.J. Komadel, J. Madejova, Acid activated clays, in: F. Bergaya, B.K.G. Theng, G. Lagaly (Eds.), Acid-Activated Clays, Handbook of Clay Science, Elsevier, Amsterdam, 2006, p. 263.
[18] F. Kooli, P.C. Hian, Q. Weirong, S.F. Alshahateet, C. Fengxi, J. Porous Mater. 13 (2006) 319–324.
[19] F. Kooli, P.C.M.M. Magussin, Clay Miner. 40 (2005) 233–243.
[20] F. Kooli, Y.Z. Khimyak, S.F. Alshahateet, F. Chen, Langmuir 21 (2005) 8717–8723.
[21] W. Xie, Z. Gao, W.K. Liu, W.P. Pan, R. Vaia, D. Hunter, A. Singh, Thermochim. Acta 367–368 (2001) 339–350.
[22] F. Kooli, Langmuir 25 (2009) 724–730.
[23] F. Kooli, W. Jones, J. Mater. Chem. 8 (1998) 2119–2124.
[24] H. He, R.L. Frost, T. Bostrom, D. Yang, Y. Xi, T. Kloprogge, Appl. Clay Sci. 31 (2006) 262–271.
[25] S.H. Xu, S.A. Boyd, Environ. Sci. Technol. 29 (1995) 3022–3028.
[26] J.M. Cervantes-Uc, J.V. Cauich-Rodriguez, H. Vazquez-Torres, L.F. Garfias-Mesias, D.R. Paul, Thermochim. Acta 457 (2007) 92–102.
[27] F. Kooli, T. Sasaki, F. Mizukami, M. Watanabe, C. Martin, V. Rives, J. Mater. Chem. 11 (2001) 841–845.
[28] Y. Okahata, A. Shimuzi, Langmuir 5 (1989) 954–959.
[29] T. Yui, H. Yoshida, H. Tachibana, D.A. Tryk, H. Inoue, Langmuir 18 (2002) 891–896.
[30] R.A. Vaia, R.K. Teukolsky, E.P. Giannelis, Chem. Mater. 6 (1994) 1017–1022.
[31] S.Y. Lee, S.J. Kim, Clay Miner. 38 (2003) 225–232.